PHYSICAL REVIEW B VOLUME 47, NUMBER 8 15 FEBRUARY 1993-II

Self-consistent calculation of the intrinsic bistability in double-barrier heterostructures

P. L. Pernas and F. Flores
Departamento de Física de la Materia Condensada C-XII, Facultad de Ciencias, Universidad Autónoma, E-28049 Madrid, Spain

E. V. Anda
Instituto de Física, Universidade Federal Fluminense, Outeiro de Sao Joao Batista s/n, Niteroi, Rio de Janeiro, Rio de Janeiro, Brazil
(Received 22 May 1992)

The intrinsic bistability of double-barrier heterostructures has been analyzed by using the nonequilibrium Keldysh formalism. In this approach, the induced electron charge in the well is calculated as a function of the applied bias and the electrostatic potential induced in the heterostructure. Self-consistency is achieved by relating this induced potential to the electron charge. Detailed results for different AlAs/GaAs/AlAs double barriers have been analyzed and show good agreement with the experimental results. A bistability behavior is found for high dopings.

I. INTRODUCTION

Resonant tunneling in multiple-barrier heterostructures has been extensively studied in the last decade due to its very interesting applications. Great improvements in the fabrication of very small and versatile devices promoted experimental and theoretical studies of the transport properties on these systems.[1,2]

The double-barrier heterostructure has been reported to present specific nonlinear phenomena which are mainly reflected in the observation of bistability in the *I-V* characteristic curve in the region in which the device exhibits negative differential resistance properties.[3,4] More recently these properties have been studied under the effect of magnetic fields showing that the bistability could be transformed into a multistable and highly amplified phenomenon.[5]

Two possible causes that could originate the hysteresis appearing in the *I-V* curve have been discussed in the literature. One is the spontaneous oscillations of an external electric circuit with negative differential resistance.[6] The second, which is the object of this paper, is an effect produced by the rapid leakage of electronic charge accumulated at the well between the barriers when the applied potential is taking the system out of resonance.[7]

This nonlinear effect should be incorporated into the equation of motion for the carriers assuming that the potential profile depends self-consistently upon the distribution of charge.[7] As is well known in the realm of nonlinear optical phenomena the multistable behavior and irreversible properties are a consequence of this nonlinear self-consistent dependence.[8]

Bistability in double-barrier heterostructures has been studied theoretically in the past few years by several authors using different techniques.[9,10] In the simplest approach, the bistability has been analyzed making a crude estimation of the space-charge buildup inside the well. In a more sophisticated treatment, a simultaneous solution of the Schrödinger and the Poisson equations has been calculated to determine the potential created by the distribution of charges. There is, however, no systematic analysis of these nonlinear problems in nanostructures as a function of the relevant parameters that determine the physical properties of the system.

Let us mention that the effect of the relaxation suffered by the electrons through the emission of phonons might be an important effect, because it certainly changes the whole distribution of charges in the system and as a consequence the bistability properties. Moreover, the interference of two or more resonant peaks that eventually changes the whole behavior of the bistability has been overlooked from the theoretical and also the experimental point of view.

II. MODEL

In this paper we analyze the transport properties of a three-dimensional double-barrier heterostructure joining two reservoirs. The nonlinear effects mentioned above are studied by introducing a full self-consistency between the potential acting on the carriers and the charge induced along the sample, although the electron-phonon relaxation mechanism has been neglected. We follow the thermodynamical nonequilibrium formalism derived by Keldysh[11] and developed later by Caroli *et al.*[12] This formalism has several advantages since the calculation of the current even in the presence of many-body effects can be obtained from one-particle Green functions that provide all the tools for obtaining in a self-consistent way the potential profile created by an external bias. The method yields all the information associated with the nonequilibrium independent-particle situation, which is the case we have analyzed in this paper. It is worth mentioning that many-body effects can be calculated in principle to all orders in perturbation theory, a case in which most of the other formalisms fail to give a rigorous and reliable answer. The model analyzed in this paper[13] consists of an infinite three-dimensional cubic system with n sites in the direction of the applied field (which has been taken to be the z axis) intercalated between two Bethe lattices that play the role of two reservoirs having chemical potentials μ_L and μ_R. We describe this model by a first-neighbor tight-binding Hamiltonian:

 ©1993 The American Physical Society

$$\hat{H}_0=\hat{H}_{\text{Bethe,left}}+\hat{H}_{\text{Bethe,right}}+\sum_{k_\parallel,i=1} E_i(k_\parallel)\hat{n}_i(k_\parallel)+\sum_{k_\parallel,\sigma,i\neq j} t_{i,j}[\hat{c}^\dagger_{i,\sigma}(k_\parallel)\hat{c}_{j,\sigma}(k_\parallel)+\hat{c}^\dagger_{j,\sigma}(k_\parallel)\hat{c}_{i,\sigma}(k_\parallel)]$$
$$+\sum_{k_\parallel} t_{0,1}[\hat{c}^\dagger_{0,\sigma}(k_\parallel)\hat{c}_{1,\sigma}(k_{k\parallel})+\hat{c}^\dagger_{1,\sigma}(k_\parallel)\hat{c}_{0,\sigma}(k_\parallel)]+\sum_{k_\parallel} t_{n,n+1}[\hat{c}^\dagger_{n,\sigma}(k_\parallel)\hat{c}_{n+1,\sigma}(k_\parallel)+\hat{c}^\dagger_{n+1,\sigma}(k_\parallel)\hat{c}_{n,\sigma}(k_\parallel)] , \quad (1)$$

where we have used the translation symmetry of the system in the direction perpendicular to the applied field to Fourier transform the Hamiltonian in $k_\parallel$; $E_i(k_\parallel)$ represents the diagonal level of the single orbital at each site along the z direction. The site dependence of the diagonal element incorporates the potential profile due to the distribution of charge within the system and the modeling of the barriers and the well of the heterostructure:

$$E_i(k_\parallel)=E_i+2t(\cos k_x a+\cos k_y a) . \quad (2)$$

The matrix elements $t_{i,j}$ correspond to the hopping between the nearest-neighbor atoms, $t_{0,1}$ and $t_{n,n+1}$ being the parameters linking the system to the Bethe lattices; in our calculation $t_{i,j}=t$. H_{Bethe} represents the Hamiltonian of a z-fold coordinated Bethe lattice.

The model is not completely determined without establishing the relation via the Coulomb interaction, between the potential induced in the system and the electron charge at each site. A linear equation has been chosen to relate these potentials to the induced charges at each site, δn_i:

$$\delta V_i=\sum_j \alpha_{i,j}\delta n_j , \quad (3a)$$

where E_i of Eq. (2) is given by

$$E_i=E_i^{(0)}+\delta V_i . \quad (3b)$$

$E_i^{(0)}$ is assumed to depend upon i in order to take into account the existence of barriers and wells in the system. Here δV_i represents the electrostatic potential induced by the charges δn_i and is measured with respect to the case of zero bias, $\alpha_{i,j}$ being given by the Coulomb interaction where the relation between the charge and the potential is screened by the semiconductor dielectric constant. For simplicity the coefficients $\alpha_{i,j}$ are defined by assuming that the charge δn_i at the i site is a planar charge extending uniformly in the direction perpendicular to the current flow.

The conductance properties of the heterostructure for a given bias are obtained by using the Keldysh[11] formalism. We calculate the retarded and the advanced Green functions $\hat{G}^R(\omega)$, $\hat{G}^A(\omega)$, and the nonequilibrium ones, $\hat{G}^{+-}(\omega)$ and $\hat{G}^{-+}(\omega)$, defined by

$$\hat{G}^{+-}_{i,j}(k_\parallel,\omega)=-i\langle\hat{c}_i(k_\parallel)\hat{c}_j^\dagger(k_\parallel)\rangle_\omega , \quad (4a)$$

$$\hat{G}^{-+}_{i,j}(k_\parallel,\omega)=+i\langle\hat{c}_i^\dagger(k_\parallel)\hat{c}_j(k_\parallel)\rangle_\omega , \quad (4b)$$

where $\langle\ \rangle_w$ represents the Fourier transform of the mean values taken on the nonequilibrium state of the system. While the imaginary part of the retarded Green function will give the density of states of the system, the spectral weight of $G^{+-}_{i,i}(\omega)$ will allow us to know how that density of states is really occupied by the electrons which due to the applied bias are out of thermodynamical equilibrium.

Following Caroli *et al.*,[12] the electrical current induced in the system is given by

$$I=\frac{2e}{h}t\sum_{k_\parallel}\int_{-\infty}^{\infty}d\omega[G^{+-}_{1,1}(k_\parallel,\omega)g^{-+}_{0,0}(k_\parallel,\omega)-G^{-+}_{1,1}(k_\parallel,\omega)g^{+-}_{0,0}(k_\parallel,\omega)] , \quad (5)$$

where the Green functions $\hat{g}(k_\parallel,\omega)$ correspond to the solution of the problem when we take in the Hamiltonian of Eq. (1) $t_{0,1}=t_{n,n+1}=0$. In this particular case the system is in equilibrium, the current is zero, and the Green functions can be obtained using standard techniques.

The dressed Green functions $\hat{G}(k_\parallel,\omega)$ can be calculated using the Dyson equations:

$$\hat{G}^R(k\|,\omega)=\hat{g}^R(k\|,\omega)+\hat{G}^R(k_\parallel,\omega)\hat{T}\hat{G}^R(k_\parallel,\omega) , \quad (6a)$$

$$\hat{G}^{+-}(k_\parallel,\omega)=[\hat{I}+\hat{G}^R(k_\parallel,\omega)\hat{T}]\hat{g}^{+-}(k_\parallel,\omega)[\hat{I}+\hat{T}\hat{G}^A(k_\parallel,\omega)] , \quad (6b)$$

where the matrix T is taken to be the hopping elements between sites 0 and 1 and sites n and $n+1$. In other words, $T=0$ represents the case with the linear chain uncoupled to the Bethe lattices. It is worth mentioning that as the system is taken from equilibrium by a one-body perturbation the self-energy can be represented by a diagonal matrix.

From this formalism the accumulated charge δn_i can be obtained from the equation

$$\delta n_i=\frac{1}{2\pi i}\sum_{k_\parallel}\int_{-\infty}^{\infty}d\omega\,\hat{G}^{+-}_{i,i}(k_\parallel,\omega)-n_i^{(0)} , \quad (7)$$

where $n_i^{(0)}$ is the background charge. Typically we take $n_i^{(0)}$ uniform in the injector and the collector up to the barriers of the heterostructure.

The solution of the problem implies the self-consistent calculation of Eqs. (6) and (7). The procedure determines the local density of states of the system at any site, the local nonequilibrium electronic occupation of the available states of the system, the potential profile seen by the carriers, and from Eq. (5) the electrical current as a function of the applied voltage.

III. RESULTS

In order to establish in a systematic way which are the relevant parameters that determine the bistability properties, we have calculated from Eq. (5) the I-V characteristic of double-barrier heterostructures for different geometries and different semiconductor dopings. In our calculations the collector and the injector are assumed to have the same doping, extending uniformly up to its corresponding barrier. In Hamiltonian (1), the levels of the

general i sites for the Bethe lattices, the well, the injector, and the collector have been taken to be the same, E_0. In the two barriers we take $E_i = E_0 + \Omega$, Ω being a constant. Moreover t has been chosen to give for the semiconductor band structure an effective mass $m^* = 0.067$, the GaAs case.

Figure 1 shows the I-V characteristic for a 48-Å well width between two 30-Å-thick barriers. The two barriers's height, Ω, has been taken to be 300 meV. Different I-V curves correspond to different dopings in the emitter and collector regions $n_d = 1.61 \times 10^{18}$, 3.46×10^{18}, and 5.74×10^{18} cm^{-3}; the Fermi energy for these electron densities are 75, 125, and 175 meV. The results of Fig. 1 show the bistability region appearing around $V \approx 160$ mV; notice that the bistable widths, 7.5, 17.5, and 2.5 mV, increase initially almost linearly with E_f, showing a saturation effect for high dopings. We should stress that in the results of Fig. 1, the bistability domain is strongly affected by the second well level for $n_d = 5.74 \times 10^{18}$ cm^{-3}. In general for high dopings there is a strong interaction between the two well levels; this interaction modifies the bistability curves. This point will be discussed further below.

Figure 2 shows the I-V characteristics for a double barrier with a 36-Å well width between an injector barrier of 18 Å and a collector barrier of 21 Å. In this case the barrier height Ω has been taken to be 500 meV. Different curves correspond to the same dopings of Fig. 1, with $n_d = 1.61 \times 10^{18}$ and 5.74×10^{18} cm^{-3}. The aim of the figure is to show how the asymmetric barrier enhances the bistability; the widths corresponding to the previous dopings are 15, 30, and 45 mV, values that represent a linear dependence with E_f.

A more important bistability enhancement is shown in Fig. 3 where we show the results for a double barrier having a 36-Å well width between an injector barrier of 18 Å and a collector barrier of 30 Å (the barrier height Ω is 500 meV). Compared with the case of Fig. 2, we have only increased the width of the collector barrier thickness. Our results show a dramatic increase of the bistability region due to the increase of the double-barrier asymmetry.[14] The bistability widths for $n_d = 1.61 \times 10^{18}$, 3.46×10^{18}, and 5.74×10^{18} cm^{-3} are 65, 105, and 125 mV, respectively. We also find for $n_d = 5.74 \times 10^{18}$ cm^{-3} that the current shows an important increase for voltages larger than 400 mV. This is again due to the effect of the second well level.

In order to analyze how the interaction between the first and second levels of the well can modify the shape of I-V curves around the bistability domain, we have shown in Fig. 4 some results for the same double-barrier dis-

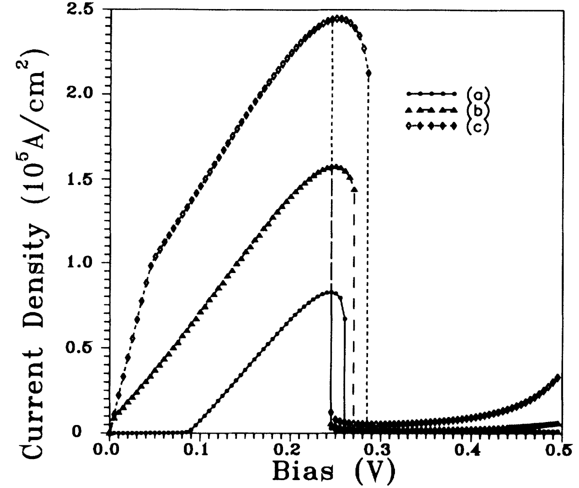

FIG. 2. As Fig. 1 for barrier height $\Omega = 500$ meV and the followings widths: injector barrier, 18 Å; well, 36 Å; collector barrier, 21 Å; (a) $n_d = 1.61 \times 10^{18}$ cm^{-3}; (b) $n_d = 3.46 \times 10^{18}$ cm^{-3}; (c) $n_d = 5.74 \times 10^{18}$ cm^{-3}.

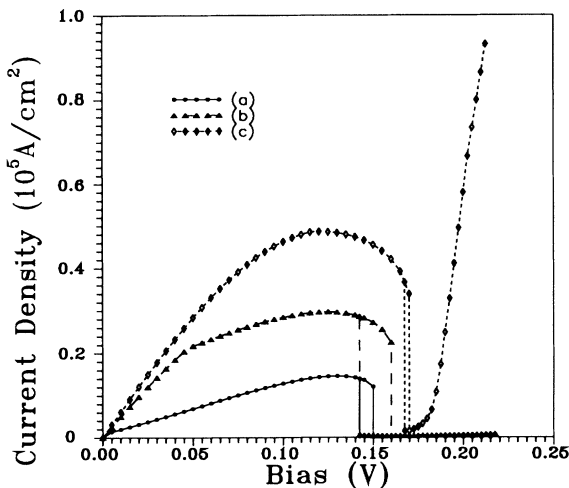

FIG 1. I-V characteristics for a double-barrier heterostructure having barrier height $\Omega = 300$ meV and the following widths: injector barrier, 30 Å; well, 48 Å; collector barrier, 30 Å; (a) $n_d = 1.61 \times 10^{18}$ cm^{-3}; (b) $n_d = 3.46 \times 10^{18}$ cm^{-3}; (c) $n_d = 5.74 \times 10^{18}$ cm^{-3}.

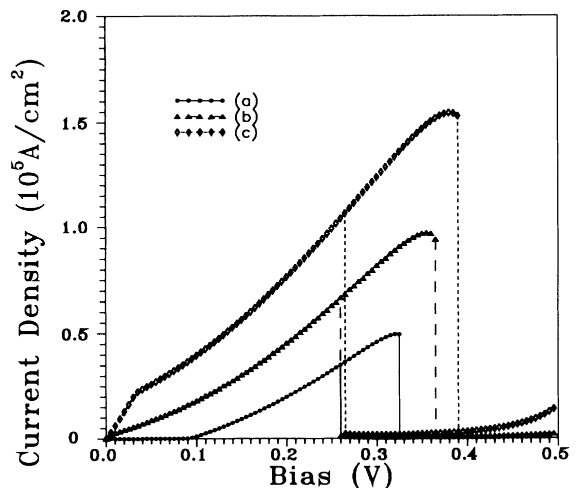

FIG. 3. As Fig. 1 for barrier height $\Omega = 500$ meV and the followings widths: injector barrier, 18 Å; well, 36 Å; collector barrier, 30 Å; (a) $n_d = 1.61 \times 10^{18}$ cm^{-3}; (b) $n_d = 3.46 \times 10^{18}$ cm^{-3}; (c) $n_d = 5.74 \times 10^{18}$ cm^{-3}.

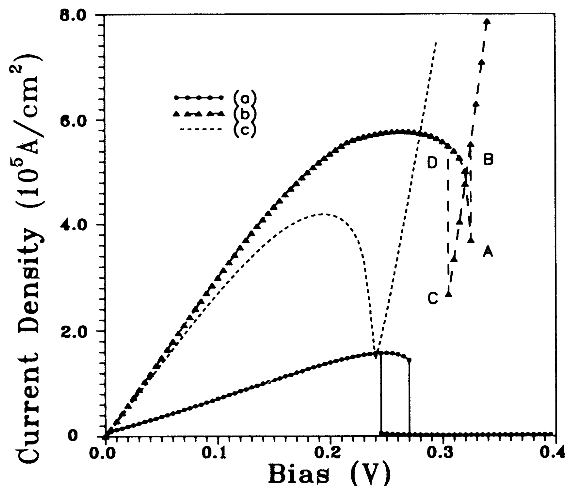

FIG. 4. I-V characteristics for the same double-barrier heterostructure of Fig. 2: (a) $n_d = 3.46\times10^{18}$ cm^{-3}; (b) $n_d = 1.45\times10^{19}$ cm^{-3}; (c) $n_d = 1.45\times10^{19}$ cm^{-3} calculated using a linear potential profile along the heterostructure.

cussed in Fig. 2. These I-V curves correspond to $n_d = 3.46\times10^{18}$ and 1.45×10^{19} cm^{-3}. The first case has also been drawn in Fig. 2, and is shown here for the sake of comparison. This case displays the typical I-V bistability curve, the same type of curve appearing in all the low-doping cases. The results for $n_d = 1.45\times10^{19}$ cm^{-3} show a bistability region presenting a feature due to the interaction between the two levels of the well. The difference between these two curves can be understood in the following way: in the usual bistability curves, the solution having smaller current has also smaller accumulation of charge, because things are only controlled by a single level that is either partially occupied or empty, depending on its position with respect to the Fermi energy. In the second case, when two levels of the well affect the bistability region, the charge in the first level decreases when it falls off from resonance. The second peak, however, has also lowered its position due to the reduction of the charge of the first level entering into the resonant region and increasing its charge. Then, in the jump $A \rightarrow B$ of Fig. 4, the system increases its current due to the resonance matching between the second level and the Fermi energy (similar things happen for the jump $C \rightarrow D$).

The results of Fig. 4, showing the strong interference between the two well levels, have been obtained for a very large doping: $n_d = 1.45\times10^{19}$ cm^{-3}. We should comment that similar results could be obtained for smaller dopings if the well width is much larger. Thus, a factor of 2 in the well thickness would reduce the well levels by a factor of 4. The bistability features could be obtained with smaller Fermi energies (reduced by a factor of 4) which represents a doping reduction of a factor of 8. This suggests that the I-V curves shown in Fig. 4 for the bistability region could be reached for well thicknesses of 80 Å with collector and injector dopings of 2×10^{18} cm^{-3}.

Finally, coming back to the results of Figs. 1–3, it is worth mentioning that our results for the normal bistability widths are in reasonable agreement with the experimental evidence.[4] Typically, for symmetric double barriers and emitter and collector dopings smaller than 10^{18} cm^{-3}, the bistability widths are smaller than 5–10 mV. These widths can be increased dramatically, however, by using asymmetric barriers; this yields bistability widths of 30 or 40 mV for 5×10^{17} cm^{-3} dopings.

In conclusion, we have presented detailed results for the bistability behavior of symmetric and asymmetric double barriers. Our results show how the bistability width depends on the geometry of the double barrier and the collector and emitter dopings. More importantly, we have shown how two different levels of the quantum well can interfere yielding a behavior of the I-V curve in the bistable region. This effect appears for relatively high emitter and collector dopings, with the Fermi energy level of the system located between the two quantum-well levels.

ACKNOWLEDGMENTS

This work was partially supported by the Spanish CICYT under Contract No. MAT 89-165. Two authors (P.L.P and F.F.) thank Dr. L. Esaki for helpful discussions.

[1]L. Esaki and R. Tsu, IBM J. Res. Dev. **14**, 61 (1970); R. Tsu and L. Esaki, Appl. Phys. Lett. **22**, 562 (1973); L. Chang, L. Esaki, and R. Tsu, **24**, 593 (1974).

[2]E. E. Mendez, L. Esaki, and W. I. Wang, Phys. Rev. B **33**, 2893 (1986).

[3]V. J. Goldman, D. C. Tsui, and J. E. Cunningham, Phys. Rev. Lett. **58**, 12 (1987); **58**, 1256 (1987); V. J. Goldman, D. C. Tsui, and J. E. Cunningham, J. Phys. (Paris) Colloq. **48**, C5-463 (1987).

[4]L. Eaves, M. L. Leadbeater, D. G. Hayes, E. S. Alves, F. Sheard, G. A. Toombs, P. E. Simmonds, M. S. Skolnick, M. Henini, and O. H. Hughes, Solid State Electron. **32**, 12 (1989); **32**, 1101 (1989).

[5]M. L. Leadbeater and L. Eaves, Phys. Scr. **T35**, 215 (1991).

[6]T. C. L. G. Sollner, Phys. Rev. Lett. **59**, 14 (1987); **59**, 1622 (1987).

[7]J. O. Sofo and C. A. Balseiro, Phys. Rev. B **42**, 11 (1990); **42**, 7292 (1990).

[8]See, e.g., A. Dorsel, J. D. McCullen, P. Meystre, E. Vignes, and H. Walther, Phys. Rev. Lett. **51**, 17 (1983); **51**, 1550 (1983); B. Macke, B. Segard, and J. Zemmouri, Physica B **175**, 271 (1991).

[9]F. W. Sheard and G. A. Toombs, Appl. Phys. Lett. **52**, 1228 (1988).

[10]H. Ohnishi, T. Inata, S. Muto, N. Yokoyama, and A. Shinbatomi, Appl. Phys. Lett. **49**, 1248 (1986).

[11]L. V. Keldysh, Zh. Eksp. Teor. Fiz. **47**, 1515 (1964) [Sov. Phys. JETP **20**, 1018 (1965)].

[12]C. Caroli, R. Combescot, P. Nozieres, and D. Saint-Jones, J. Phys. C **4**, 916 (1971).

[13]P. L. Pernas, A. Martin-Rodero, and F. Flores, Phys. Rev. B **41**, 8553 (1990).

[14]V. J. Goldman and J. E. Cunningham, Solid State Electron. **31**, 731 (1989).